FRICTION IDENTIFICATION AND COMPENSATION IN A DC MOTOR

T. Tjahjowidodo, F. Al-Bender, H. Van Brussel

Mechanical Engineering Department
Division PMA, Katholieke Universiteit Leuven
Celestijnenlaan 300B, B3001 Heverlee, BELGIUM
tegoeh.tjahjowidodo@mech.kuleuven.ac.be

Abstract: Friction modeling and identification is a prerequisite for the accurate control of electromechanical systems. This paper considers the identification and control of friction in a high load torque DC motor to the end of achieving accurate tracking. Model-based friction compensation in the feedforward part of the controller is considered. For this purpose, friction model structures ranging from the simple Coulomb model through the recently developed Generalized Maxwell Slip (GMS) model are employed. The performance of those models is compared and contrasted in regard both to identification and to compensation. It turns out that the performance depends on the prevailing range of speeds and displacements, but that in all cases, the GMS model scores the best.

Keywords: motor, friction, control, compensation, precision, feedforward, feedback, hysteresis, sliding

1. INTRODUCTION

The problem of accurate control of electromechanical systems is very important in many industrial applications where such devices, e.g. motors, are themselves, or form essential parts of, positioning /tracking systems. In this paper, we consider a DC motor driving an inertial load with the aim of identifying and compensating the friction disturbances arising from the ball bearings.

A DC motor consists of two sub-processes: electrical and mechanical. The electrical sub-process consists of armature inductance, armature resistance and the magnetic flux of the stator. A second sub-process in the motor is a mechanical one. It consists of the inertia of the motor and a load (J). The difference in motor speed is caused by the electromagnetic moment generated by the amplifier current (τ_m), load (τ_0) and friction of the motor (τ_f). The electrical sub-process will not be discussed in this paper, which will deal with the identification, modeling and compensation of the friction in the ball bearings of the motor.

In the literature, identification of friction in a motor system usually considers only classical friction models, such as Coulomb and viscous friction. Pre-sliding motion, which is apparent in many friction investigations (Prajogo, 1999), is usually neglected. However, the Coloumb model defines the friction force only for $v \neq 0$; when $v=0$ the characteristic simply sets the friction force below the static force value, where v represents velocity. This makes the model quite complex to simulate, since it requires accurate detection of the velocity zero crossing. It is also impractical for friction compensation at motion stop and reversal, where the effect of stick-slip motion arises. In fact, motion never starts or stops abruptly and micro-sliding displacements are actually observed (Armstrong-Hélouvry, 1991).

Two different friction regimes have been distinguished in the literature: the pre-sliding regime, where the friction force appears predominantly as a function of displacement; and the sliding regime, where the friction force is a function of sliding velocity (Armstrong-Hélouvry, 1991, Canudas de Wit et al., 1995, Swevers et al., 2000, Al-Bender et al., 2004). The pre-sliding regime is taken into account in some advanced models, such as LuGre model, the Leuven model and the most recent Generalized Maxwell-Slip (GMS) model. The LuGre model offers a smooth transition of motion from pre-sliding to sliding regime and vice versa. However, it

does not accommodate the unique behavior of pre-sliding faithfully. In fact, the friction force shows hysteresis behavior with nonlocal memory in that regime (Prajogo, 1999, Swevers et al., 2000). The Leuven model succeeded in including this type of hysteresis, but introduced some modelling complexities and difficulties (Swevers et al., 2000, Lampaert et al., 2002). Finally, the GMS model manages to overcome those difficulties by modeling friction as a Maxwell-Slip model where the slip elements satisfy a certain, new state equation. As a result, the GMS model is able to predict not only the friction behavior in pre-sliding regime with nonlocal memory hysteresis, but also the friction force in sliding regime, which behaves in a similar way to that in the LuGre model.

An important feature in the friction identification procedure in this paper is that we will use only a single set of experiments to identify all the unknown parameters together, using a suitable optimization method, namely the Nelder-Mead Simplex algorithm.

Once the friction models have been optimized, position control incorporating friction compensation is performed. For this purpose, the inertial force and friction behavior are compensated for using a feedforward control, while a simple (PID) feedback part is included to track set-point changes and to suppress unmeasured disturbances.

In the following, section 2 formulates the DC motor torque balance, and outlines the friction models used in this investigation. Section 3 describes the experimental apparatus, while section 4 discusses the identification procedure. The identification results are discussed in section 5. Thereafter, the friction compensation scheme is sketched in section 6, while the compensation results are discussed in section 7. Finally, appropriate conclusions are drawn in Section 8.

2. MOTOR TORQUES

In general, a DC motor can be viewed as a black box with two inputs: current and load torque, and an output angular displacement (or velocity). Torque balance for a DC motor can be written as:

$$\tau_m = \tau_i + \tau_f + \tau_0 , \qquad (1)$$

where τ_m is the motor torque generated by the amplifier current, τ_i is the inertial torque from motor armature and shaft, τ_f is the friction torque and τ_0 is the load torque.

Due to the limitation of the amplifier current in the motor, it can be shown that the motor torque $\tau_m = K_m \, sat(i, i_{sat})$; and the inertial torque $\tau_i = J_m \ddot{\theta}$. Motor torque is bounded due to the current saturation limit of the servo amplifier. The saturation function is represented by $sat(i, i_{sat})$, where it has a constant value for $|i| > i_{sat}$; and it has a slope of 1 for $|i| \le i_{sat}$.

As for the friction torque τ_f in equation (1), which is our main concern, several models were used as described below.

1.1 Coulomb Friction

The classical Coloumb model of friction is described by a discontinuous relation between the friction force and the relative velocity between the rubbing surfaces. In this model, when the mass that is subjected to friction is slipping, the friction force will remain constant until the motion is reversed.

1.2 Stribeck Friction

The Stribeck friction consists of (i) a function s(v) that is decreasing in the velocity and bounded by an upper limit at zero velocity equal to the static friction force F_s, and a lower limit equal to the Coulomb force F_c., and (ii) a viscous friction part. In this approach, the constant portion of the Coulomb model is replaced by Stribeck function. Moreover, in order to overcome the jump discontinuity of the Coloumb model, at v=0, that jump is replaced by a line of finite slope, up to a very small threshold ε, as shown in Figure 1.

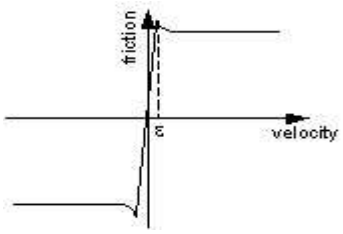

Figure 1. Friction curve of Stribeck models

1.3 LuGre Friction

The above two methods have proven to be impractical for friction compensation at motion stop and inversion, where the worst effects due to friction, namely stick-slip motion, could arise. Motion never starts or stops abruptly and pre-sliding displacements are actually observed (Prajogo, 1999, Swevers et al., 2000). Consequently, two different friction regimes can be distinguished, i.e. the pre-sliding and the gross sliding regimes, as explained in section 1. The LuGre model (Canudas de Wit et al., 1995) was the first formulation that could effect a smooth transition between those two regimes, i.e. without recourse to switching functions. It, furthermore, accounts for other friction characteristics such as the breakaway force and its dynamics. The model achieves this by introducing a state variable, representing the average deflection of elastic bristles (representing surface asperities) under the action of a tangential force, together with a state equation, governing this variable's dynamics and friction equation.

The LuGre model is very popular in the domain of control and simulation of friction due to its simplicity and the integration it affords of pre-sliding and sliding into one model. However, it has been subjected to important criticism (Swevers et al., 2000) in regard to its failure to model pre-sliding/pre-rolling hysteresis with nonlocal memory. The latter authors proposed an extension in form of the Leuven model and a subsequent improvement (Lampaert et al., 2002), however, not without introducing further difficulties.

1.4 GMS Friction

The Generalized Maxwell-Slip (GMS) friction model (Al-Bender et al., 2004, Lampaert et al., 2003) is a qualitatively new formulation of the rate-state approach of the LuGre and the Leuven models. The GMS model retains the original Maxwell-slip model structure (see e.g., Iwan, 1966), which is a parallel connection of different elementary slip-blocks and springs, but replaces the simple Coulomb law governing each block, by another state equation to account for sliding dynamics. Thus, the friction force is given as the summation of the outputs of the N elementary state models. The dynamic behavior of each elementary block is represented by one of two equations (in which F_i is the elementary friction force, k_i is the elementary spring constant, and v is the velocity):

- If the model is sticking:

$$\frac{dF_i}{dt} = k_i v \; ; \qquad (2)$$

- If the model is slipping:

$$\frac{dF_i}{dt} = sgn(v) \cdot C \cdot \left(\alpha_i + \frac{F_i}{s(v)} \right) \qquad (3)$$

Each elementary model (or block) corresponds to a generalised asperity in the contact surface, where it can stick or slip. The asperity will slip if the elementary friction force equals the maximum value $W_i = \alpha_i \, s(v)$ that it can sustain. In this regime, equation (3) will characterize the friction behavior. Once the model is slipping, it remains slipping until the direction of movement is reversed or its velocity approaches zero value. When the asperity is sticking the elementary model will act as a spring with stiffness of k_i.

3. EXPERIMENTAL SETUP

Experimental identification of friction in a DC motor was performed on ABB motor type M19-S, with maximum rated torque of 0.49 Nm/amp and armature inertia of 0.001 kgm^2. To allow a straightforward position and velocity data collection on the motor, an incremental angular encoder was connected to the shaft through a toothed belt and pulleys. The pulleys give a reduction ratio of 1:3 to increase the sensitivity of the encoder, whose resolution is 5000 pulses per revolution. Figure 2 shows a schematic of the experimental setup.

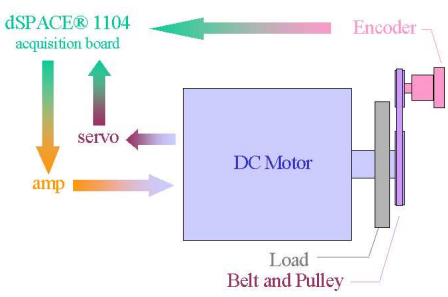

Figure 2. Schematic of the setup

4. IDENTIFICATION OF FRICTION MODELS

The identification experiment was carried out by applying an input velocity signal. A special input command was designed for this purpose. This command signal is composed of a band limited random signal with cutoff frequency of 4 Hz, which is enveloped by a certain signal. This envelope signal is composed of the three first non-zero terms of the Fourier series of a rectangular signal, which has period of 10 seconds. The purpose of enveloping this input signal is to emphasize the behavior of presliding friction in the experiment, which corresponds to the friction at low velocity and low displacement. The signal and its corresponding envelope signal are shown in Figure 3. These signals were applied through a dSPACE-1104 acquisition card to the servo amplifier. The real current input to the motor, which is assumed to correspond to the torque was measured and recorded using the same acquisition unit.

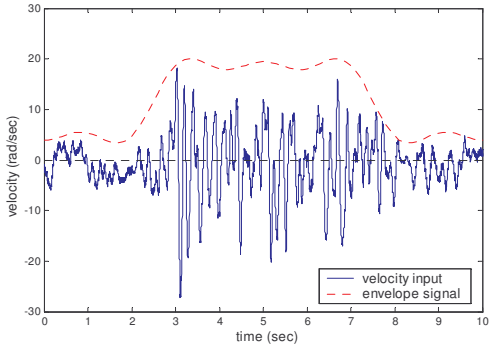

Figure 3. Velocity input signal

5. IDENTIFICATION RESULTS

Fifty thousand points, at one millisecond time sampling, were collected for each test. The first 10 seconds were used as a training set and the remaining 40 seconds were used as testing set. The Nelder-Mead Simplex algorithm was used for optimizing the parameters in each model.

Since the system being identified here is (highly) nonlinear, error quantification techniques pertaining to linear systems, such cross-correlation between input, output and residuals, etc., cannot be used.

Instead, as a measure of performance, the normalized mean square error was used, which is defined by:

$$\mathrm{MSE}(\hat{y}) = \frac{100}{N\sigma_y^2} \sum_{i=1}^{N} (\hat{y}_i - y_i)^2 \qquad (4)$$

where y is the output (in this case is the friction force), σ_y^2 is its variance and the caret denotes an estimated quantity.

The performance values can be seen in Table 1. The values between brackets represent the peak-to-peak errors that are normalized by the RMS value of the actual torques. In this table the performances are divided into two groups, one for high velocities and the other for low velocities. Each group is calculated based on its envelope signal. High velocity

performance values are calculated at the instances when the envelope velocity is high, and low velocity performance values are calculated when the envelope velocity is low.

The estimated torques of the modeling technique and the measured torque are shown in Figure 4, for Coulomb, Stribeck-Coulomb, LuGre and GMS (with 4 elements), from left to right and top to bottom respectively. It can be clearly seen that the identification results of the classical friction models fall far from the actual value in some regions, especially in the low velocity regions (approximately before time 3 seconds), which have lower angular displacement, i.e. more pre-sliding regime portion.

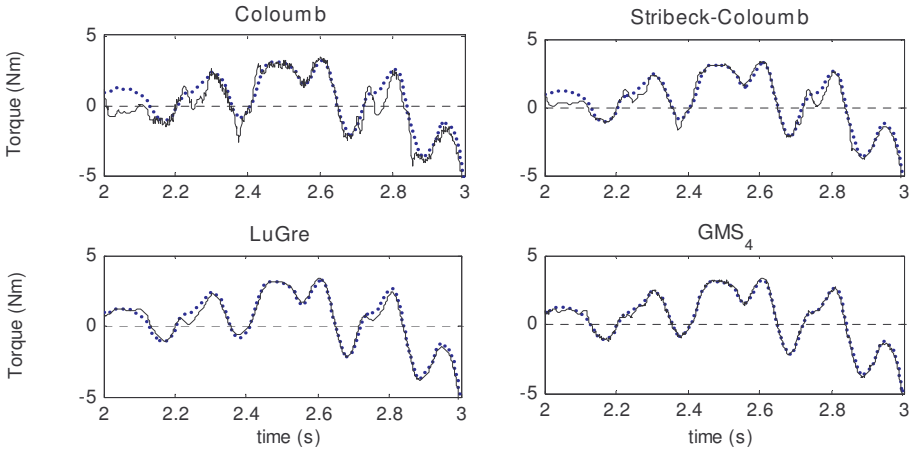

Figure 4. Measured and estimated torques for different models. Dotted lines represent the measured torques, and solid lines are the estimated torques.

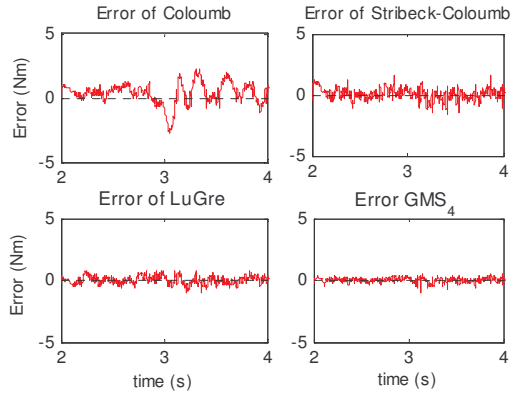

Figure 5. Error of the estimated torques

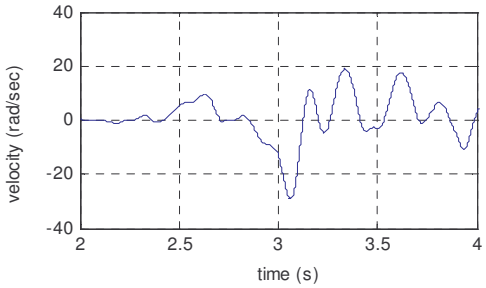

Figure 6. Velocity signal in the validation set

On the other hand, the results of the two recent models, LuGre and GMS, show much better performance. They give significant improvements, especially in the low velocity region, for which the classical models could not account well.

The most recent friction model, GMS, gives the best results in this experiment. In particular, strong improvement is achieved in the low velocity region. The ability to estimate the friction behavior in pre-sliding regime is shown as the superiority of the GMS model, while it does not lose its ability to estimate the friction in the gross sliding regime. These results are summarized in Table 1.

As a comparison, another identification utilizing GMS model with higher number of Maxwell-Slip elements was conducted. In this identification, 10 Maxwell-Slip elements were used, instead of 4. Although this gives a slightly better result, the improvement is not significant as shown in the last row of Table 1. Increasing the Maxwell-Slip by 6 elements means adding twice times six (=12) parameters in the optimization process, which is a high price for the slight improvement.
The error of the corresponding models and the velocity input signal are shown in Figure 5 and Figure 6 respectively.

Table 1. Performances of identification result for high frequencies experiment

	High velocity MSE (max. err.)	*Low velocity* MSE (max. err.)
Coulomb	4.00% (0.6757)	17.92% (1.2993)
Stribeck	0.55% (0.2762)	9.59% (1.2604)
LuGre	0.41% (0.2440)	4.30% (0.6466)
GMS_4	0.40% (0.2350)	1.39% (0.5711)
GMS_{10}	0.38% (0.2300)	1.19% (0.5177)

6. FRICTION COMPENSATION SCHEME

In this section, position control incorporating friction compensation using the aforementioned models in the feedforward will be described. For this purpose, the inertial force and the friction force, as modeled in the previous section, are

included in the feedforward loop. The control scheme is depicted in Figure 7.

The feedback loop, which is required to track set-point changes and to suppress unmeasured disturbances, is chosen to be a PID controller with gains K_p = 200 Nm/rad, K_i = 0 Nm/rad.s, and K_d = 0.15 Nm.s/rad. In order to obtain a consistent comparison, these gains were optimized for one of the control schemes, namely that employing LuGre compensation, and used with the same values for all the other models. As a numerical quantification of the validation criterion, the peak-to-peak tracking error will be used for different reference input signals.

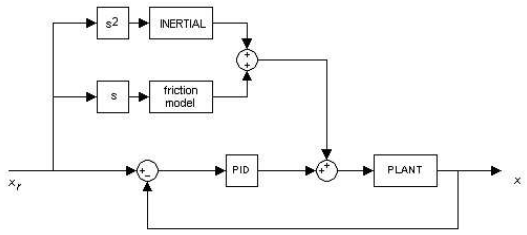

Figure 7. The feedforward/feedback control scheme for friction compensation

7. COMPENSATION RESULTS

Two different reference signals were employed to validate the friction compensation. The first reference position signal is a filtered random signal with a very small stroke in order to emphasize the pre-sliding regime of the friction torque. The reference signal was generated using a random signal generator, which is passed through a low pass, 4th order digital Butterworth filter with 1 Hz cutoff frequency. The tracking error of each friction compensation model can be seen in Figure 8. (All these results were obtained with the same PID controller parameters). The numerical RMS values are given in Table 2.

Friction compensation based on the Coloumb model yields large errors, and is almost identical to the scheme that has no feedforward compensation. Since the reference signal has a very small stroke and it is emphasizing the presliding regime, the Coulomb model is merely playing on its threshold region. Thus, the Coulomb model will act only as a gain to the reference signal. The GMS model compensation, in contrast, gives significant improvement in comparison with the other models. It shows superiority at the reversal points compared to the LuGre model. The jumps in the tracking error of the LuGre model, which correspond to the sticking problem, are significantly reduced in the GMS compensation model.

Table 2. Performances of friction compensation for a low stroke random input

Compensation	*RMS (rad x1000)*
No Feedforward	5.6
Coulomb	5.3
LuGre	1.6
GMS	0.6

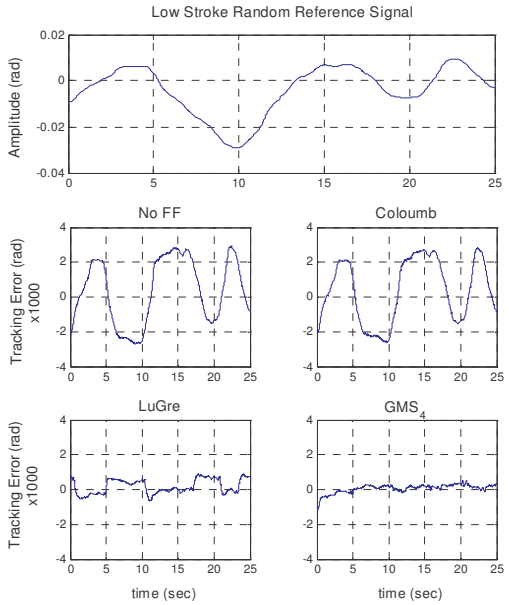

Figure 8. The tracking errors for low stroke filtered random reference input. The top-left figure shows the tracking error for a system with no feedforward friction compensation. In the top-right figure, the Coulomb friction was used as a feedforward friction compensation, while the bottom figures show the friction compensation results using the LuGre and the GMS model.

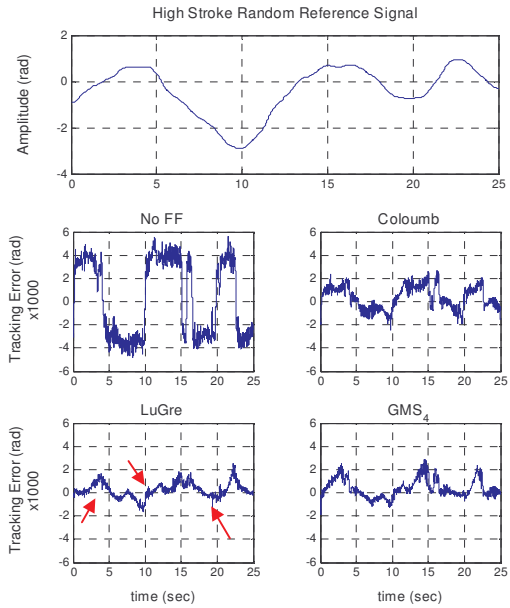

Figure 9. The tracking errors for high stroke filtered random reference input. The top-left figure shows the tracking error for a system with no feedforward friction compensation. In the top-right figure, the Coulomb friction was used as a feedforward friction compensation, while the bottom figures show the friction compensation results using the LuGre and the GMS model.

The second reference signal used in this experiment is a filtered random signal similar to the signal in the previous experiment, except that this signal has larger amplitude. The maximum stroke of this

random signal was set to π rad (or half of the shaft's rotation). In this case, the pre-sliding friction is not expected to dominate the overall behavior.

The tracking errors for each compensation scheme are depicted in Figure 9. For this desired position signal, the GMS model again gives the best performance. Nevertheless, according to the performance values in Table 3, it does not give a significant improvement compared to the LuGre model, even though the spikes in the tracking error, which are indicated by the arrows in the figure, are obviously reduced. These results are understandable, since the system was excited with a high stroke, i.e. more in sliding regime than in pre-sliding regime. In this case, the zero crossings of the velocity, where the pre-sliding regime friction arises, will occur only over a very short portion during the whole motion.

Table 3. Performances of friction compensation for a high stroke random input

Compensation	*RMS (rad x1000)*
No Feedforward	10.5
Coulomb	5.7
LuGre	4.7
GMS	4.6

8. CONCLUSION

The following conclusions can be drawn from this investigation:

- Friction identification using a single experiment is possible to conduct, even for the more complex and 'more' nonlinear models. Friction identification utilizing the most recent GMS model, which incorporates two regimes of friction, was also possible to conduct using a single experiment. However, selection of the excitation signal plays an important role for identification using single experiment.
- For motions with high velocities, the classical models such as Coulomb friction and the Stribeck friction model give satisfactory results comparable to the advanced models. However, at low velocities, which emphasize the pre-sliding regime, the classical models fail to give a satisfactory estimation of the overall friction. For a good estimation in pre-sliding, models that incorporate hysteresis behavior are necessary.
- The ability to estimate the friction behavior in pre-sliding regime is the superiority of GMS model, while it does not lose its ability to estimate the friction in sliding regime. Therefore the GMS model can capture friction behavior for any working range of displacement and velocity.
- The nonlinear effect of friction in a high load torque DC motor is successfully compensated for in a feedforward based control experiment. In all of the validation cases, the GMS model yields the best results. This can be understood since this (most recent model) accommodates the hysteresis behavior with non-local memory for the presliding regime friction, while modeling the gross sliding also.

ACKNOWLEDGEMENT

The authors wish to acknowledge the partial financial support of this study by the Volkswagenstiftung under grant No. I/76938.

REFERENCES

Al-Bender, F., V. Lampaert and J. Swevers (2004). Modeling of Dry Sliding Friction Dynamics: From Heuristic Models to Physically Motivated Models and Back, *Chaos: An Interdisciplinary Journal of Nonlinear Science*, **14**, 2, 446-460.

Armstrong-Hélouvry, B. (1991). Control of Machines with friction, Kluwer Academic Publishers.

Canudas de Wit, C., H. Olsson, K.J. Åström and P. Lischinsky (1995). A new model for control of systems with friction. *IEEE Trans. Automat. Contr*. **40**, 3, 419-425.

Dahl, P.R. (1968) A solid friction model, Tehc. Rep. TOR-158, *The Aerospace Corporation, El Segundo*, CA, 3107-18.

Iwan, W.D. (1966). A distributed-element model for hysteresis and its steady-state dynamic response, *Journal of Appl. Mech*., **33**, 4, 893-900.

Lampaert, V., J. Swevers and F. Al-Bender (2002). Modification of the Leuven Integrated Model Structure, *IEEE Trans. Automatic Contr.* **47**, 4, 683-687.

Lampaert, V., F. Al-Bender and J. Swevers (2003). A Generalized Maxwell-Slip Friction Model Appropriate for Control Purposes, *Proc. of the 2003 International Conference on Physics and Control*, Saint-Petersbourg, Russia, 1170-1178

Parlitz, U., A. Hornstein, A. Engster, F. Al-Bender, V. Lampaert, T. Tjahjowidodo, S.D. Fassois, D. Rizos, C.X. Wong, K. Worden and G. Manson (2004). Identification of Presliding Friction Dynamics, *Chaos: An Interdisciplinary Journal of Nonlinear Science*, **14**, 2, 420-430.

Prajogo, T. (1999). Experimental Study of Pre-rolling Friction for Motion-Reversal Error Compensation on Machine Tool Drive Systems. PhD thesis, Department Werktuig-kunde Katholieke Universiteit Leuven, Belgium.

Swevers, J., F. Al-Bender, C.G. Ganseman and T. Prajogo (2000). An integrated friction model structure with improved presliding behavior for accurate friction compensation. *IEEE Trans. Automat. Contr*. **45**, 4, 675-686.

Vrančić, D., Đ. Juričić and T. Höfling (1994). Measurements and mathematical modeling of a DC motor for the purpose of fault diagnosis, *Institute of Automatic Control, Technical University of Darmstadt,* Germany.